Estuarine, Coastal and Shelf Science 131 (2013) 297–309

Contents lists available at ScienceDirect

Estuarine, Coastal and Shelf Science

journal homepage: www.elsevier.com/locate/ecss

Monsoon sedimentation on the 'abandoned' tide-influenced Ganges–Brahmaputra delta plain

Kimberly G. Rogers [a,*], Steven L. Goodbred Jr. [a], Dhiman R. Mondal [b,1]

[a] Department of Earth and Environmental Science, Vanderbilt University, PMB 351805, 2301 Vanderbilt Place, Nashville, TN 37235-1805, USA
[b] Department of Geology, Dhaka University, Kurzon Hall, Dhaka 1000, Bangladesh

ARTICLE INFO

Article history:
Received 23 March 2013
Accepted 17 July 2013
Available online 29 July 2013

Keywords:
Bangladesh
Ganges–Brahmaputra River
Sundarbans
mangroves
deltaic sedimentation
sea level changes
radioisotopes

ABSTRACT

Annual sediment delivery by the Ganges and Brahmaputra rivers to the Bengal margin has kept pace with sea level rise since the mid Holocene, sustaining subaerial growth of the delta. However, the Sundarbans region of the tidal delta is disconnected from major distributary sources of sediment and is often thought to be sediment starved, eroding, and susceptible to the meter of sea level rise predicted for the 21st century. Despite these assumptions, direct sedimentation measurements on the tidal delta plain reveal widespread mean annualized accretion rates of ~1.1 cm yr^{-1}, although heterogeneous depositional patterns indicate that topography and internal creek networks influence local sediment distribution. Short-lived radioisotope inventories (^{7}Be: $t_{1/2}$ = 53.3 days) measured on the freshly accumulated sediments indicate that about ½ of the mass deposited on the lower delta was sourced directly from the seasonal flood pulse of the river; the remaining ½ is derived from older (≥1 yr) reworked sediments. Net sedimentation on this part of the delta traps ~10% of annual Ganges–Brahmaputra sediment load, with accretion rates roughly equivalent to the mean regional rate of relative sea-level rise (RSLR) of ~1.0 cm yr^{-1}. If these sedimentation rates are representative of longer-term trends and subsidence rates remain stable over the next century, the lower delta plain may continue to maintain its elevation and stability despite documented mangrove retreat around its seaward edges.

1. Introduction

Sediment delivery to low-lying coastal zones must keep pace with, if not exceed, relative rates of sea level rise in order to maintain a positive surface elevation (French, 1983; Morris et al., 2002). The Ganges–Brahmaputra River delta in Bangladesh has been cited by the Intergovernmental Panel on Climate Change as an example of a coastal system that could be flooded by the combination of rapid eustatic and regional sea level rise within the next century (Cruz et al., 2007). Approximately ¾ of the billion tons of Himalayan sediment annually transported to the Bengal basin during the southwest monsoon reaches the mouth of the Ganges–Brahmaputra River (Goodbred and Kuehl, 1999). Comprised mostly of silts and fine sands, the coarser fractions are deposited at the estuary mouth and near shore, while the finer-grained load is partitioned on the shelf between the prograding subaqueous clinothem and the rapidly accumulating Swatch of No Ground (SoNG) canyon (Eysink, 1983; Kuehl et al., 1997). Previous sediment budgets based on stratigraphy and geochronology estimate that ~400 million tons of the fluvial sediment load is distributed to the topsets and foresets of the subaqueous delta, and the remaining 350 million tons delivered to the coast bypass the shelf to the deep sea by way of the shallow-headed SoNG canyon (Kuehl et al., 1997; Allison, 1998). However, these budget calculations did not consider sedimentation and storage on the 'abandoned' tidal delta plain.

Delta plains maintain their elevation above sea level principally through sediment delivery from overbank flooding of rivers and distributaries, though the Sundarbans region of the Ganges–Brahmaputra (G–B) delta has not had direct input from the main stem river since the mid to late Holocene (Fig. 1). This part of the delta formed after 5 ka and has been gradually cut off from the main trunk and tributary channels due to eastward shifting of the G–B river courses, effectively creating an 'abandoned delta lobe' (Allison et al., 2003). Subsequent siltation of smaller distributaries that have historically delivered sediment to the lower delta has further reduced riverine input to the Sundarbans in recent decades (Chowdhury, 1966). Through the late Holocene, this general separation from

* Corresponding author. Present address: Institute of Arctic and Alpine Research, University of Colorado, 1560 30th Street, UCB 450, Boulder, CO 80309, USA.
E-mail addresses: kgrogers@colorado.edu, berly1@gmail.com (K.G. Rogers), steven.goodbred@vanderbilt.edu (S.L. Goodbred), dhimandu@gmail.com (D.R. Mondal).
[1] Present address: The City University of New York, 65-30 Kissena Blvd., Queens, NY 11367, USA.

0272-7714/$ – see front matter © 2013 Elsevier Ltd. All rights reserved.
http://dx.doi.org/10.1016/j.ecss.2013.07.014

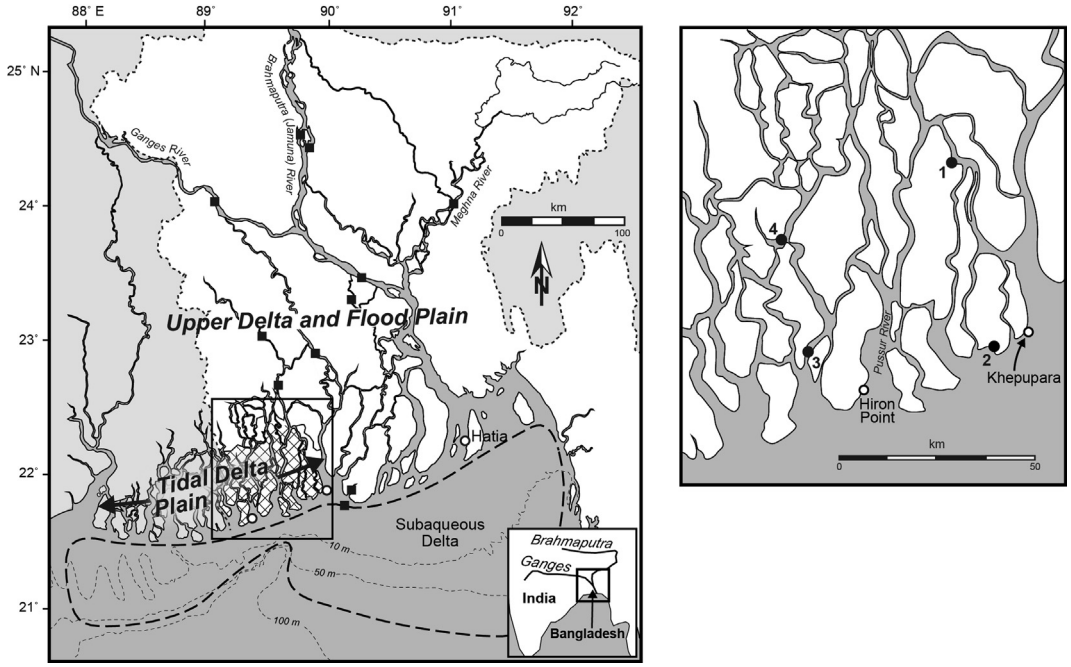

Fig. 1. Map of Ganges–Brahmaputra compound delta system, including the approximate extent of the subaqueous delta on the inner shelf. Inset is close up of the tidal delta plain that is the focus of this study. Anchor stations (marked with numbers) all lie within the boundaries of the Sundarbans National Preserve, the world's largest littoral mangrove forest. Solid squares mark locations of suspended sediment sampling during 2006 peak discharge. Open circles mark tide gauge stations mentioned in the text. Cross-hatched area marks the approximate boundary of the Bangladesh Sundarbans.

the main G–B fluvial system has curbed progradation of the Sundarbans delta plain and led to a dominance of tidal processes. Despite these patterns of 'abandonment' from main river mouths, vertical sediment accretion has been inferred on the lower delta plain using ^{137}Cs radionuclide geochronometry, with estimated decadal-scale accretion rates of ~1.1 cm yr^{-1} (Allison and Kepple, 2001).

The findings of Allison and Kepple (2001) prompt a reevaluation of the earlier sediment budget for the G–B delta by demonstrating that sediment discharged to the inner shelf is partitioned not only among the subaqueous delta and SoNG canyon, but also to the Sundarbans region of the lower delta plain. Allison and Kepple (2001) further note that radionuclide activities are very low in the lower delta plain, for example rendering ^{210}Pb ineffective for calculating accretion rates. As a result, accretion rates were estimated using less than ideal results from fallout ^{137}Cs activities, which are ordinarily used to verify sedimentation rates calculated from down-core decay profiles of ^{210}Pb. They speculate that these low activities result from dilution with older sediments eroded from the shelf, but state more information is needed to validate this interpretation and the overall accretion rates. In general, though, the results of Allison and Kepple (2001) show decreasing sedimentation rates with distance inland from the shoreline, indicating that sediment is likely sourced from the marine side and is probably introduced through tidal inundation, the seasonal monsoon set-up of sea level, and storm surges. While this earlier study used radioisotope geochronology to determine accretion rates and spatial trends of sediment input, these important results remain unconfirmed. The source of sediments accumulating on the lower delta plain and the timing of their deposition remain central questions as well. Furthermore, sampling by Allison and Kepple (2001) was limited to within 100 m of tidal channel banks "because of the presence of tigers" in the Sundarbans forest reserve.

Expanding the spatial control of sedimentation rates estimated by earlier work, the present study examines accretion patterns across intertidal islands of the Sundarbans, up to 450 m from channel banks, using both direct measurements and short-term radionuclide geochronology. Accretion rates are measured from the shoreline to 50 km inland along the tidal continuum and from the lower-salinity eastern and higher-salinity western portions of the Sundarbans using sediment traps to measure mass accumulation over a single monsoon season. Sediment accumulation values are coupled with identification of sediments sourced directly from the seasonal riverine flood pulse using ^{7}Be, a short-lived cosmogenic fallout radioisotope ($t_{1/2}$ = 53.3 days), demonstrated to be an effective tracer of terrestrial sediment discharged to marine environments (Sommerfield et al., 1999; Mullenbach and Nittrouer, 2000). ^{210}Pb is used in conjunction with ^{7}Be to identify the transport history of sediments aggrading in the Sundarbans. The combined use of direct measurements and radionuclides represents a novel approach to quantifying seasonal-scale sediment accumulation and fingerprinting sediments delivered to the 'abandoned' lower delta plain to determine their source.

2. Study area

The lower G–B delta plain is a tide-influenced depositional system containing a complex network of estuaries and islands dissected by tidal channels. River discharge is controlled by the tropical southwest monsoon, with highest rainfall and ~95% of the sediment load delivered to the coast from May–September (Coleman, 1969; Goodbred, 2003). The lower G–B delta can be further divided into a river-influenced eastern reach with major distributaries that flood annually during high discharge, and an older 'abandoned' portion of the delta to the west that is no longer connected to significant upstream river sources. This western portion of the lower delta, here referred to as the tidal delta plain, has been thought to be sediment starved similar to the abandoned lobes of other delta systems (e.g., Mississippi, [Coleman et al., 1998]; Yellow [Xue, 1993]). Reduced sediment and freshwater

input has caused the western lower delta to evolve from a distributive channel network into a system of interconnected headless tributive tidal channels.

The tidal delta plain is vegetated by the world's largest littoral mangrove forest, the Sundarbans National Preserve, a UNESCO World Heritage site. Shared by India and Bangladesh, the Sundarbans is a largely pristine mangrove ecosystem that is home to several threatened plant and animal species (including the Royal Bengal Tiger) and imparts protection from storm surges caused by tropical cyclones that recur on sub-decadal time scales in the Bay of Bengal (Giri et al., 2007). As such, the Sundarbans contribute critically important ecological and societal benefits to the region. Over 10,000 km of navigable tidal creeks ranging from a few meters to several kilometers wide traverse the Sundarbans and are maintained by semi-diurnal meso-tides (2–4 m) and the associated tidal prism. The large tidal range and funnel-shaped channel geometries generate asymmetrical flood-dominant tides that increase by ~1 m from the coast to 100 km inland. A 3–7 km-wide tidal channel known as the Pussur River serves as the general boundary between the eastern and western portions of the Sundarbans used in this study. Land elevation surveys in the Sundarbans also indicate that the eastern (western) mangrove platform averages 2.0 ± 0.9 (1.5 ± 0.8) m above mean low water levels (Ellison et al., 2000). Considering these elevations against the 2–4 m tidal range, much of the eastern Sundarbans only floods during the highest dry-season spring tides and more regularly during the monsoon-season high tides when sea-level is locally setup by onshore wind stresses (Somayajulu et al., 2003). By contrast, the mean elevation of the western Sundarbans is 0.5 m lower than mean high water, indicating there is year-round inundation of the mangrove platform during most high tides.

An important characteristic of the Bengal coast is the 60–80 cm seasonal set up of mean sea level produced by strong onshore winds during the summer monsoon (May–September) (Fig. 2). This seasonal enhancement of water level by coastal set-up is an important component of defining the intertidal zone throughout the Sundarbans. Although the rivers do not directly flood the tidal delta plain, tides overprinted by the summer monsoon set-up leads to increased inundation depths and more widespread flooding of the Sundarbans, particularly in the low-lying western area. The seasonal set up also corresponds with high river discharge and peak sediment loading at the coast. High suspended sediment concentrations are maintained year-round on the inner shelf by bed shear and vertical mixing caused by strong tidal currents west of the active river mouth (Barua et al., 1994). These persistent sediment plumes can be observed in satellite images to extend up to 100 km offshore to the topset–foreset rollover near 20 m water depth. This broad, turbid inner-shelf region is connected to the tidal delta plain by onshore propagation of the tide wave, which combined with sea level set up and high suspended sediment concentrations, enables sediments on the inner shelf to be transported far inland of the coast.

3. Methods

This study uses data gathered from the G–B tidal delta plain through sediment traps and radioisotope geochemistry. Radionuclide measurements are also made on suspended sediments collected from the upstream fluvial system, the inner shelf, and tidal creeks of the lower delta plain.

3.1. Sampling strategy

In March 2008, 48 sediment traps were placed within the boundaries of the Bangladesh portion of the Sundarbans tidal delta plain (Fig. 1). A nested sampling strategy was used, involving four main study areas that each included several sampling transects extending from the channel margin to several hundred meters inland. The four study areas (or anchor stations) are located east and west of the Pussur River, both near the coast and ~50 km inland, bounding an area of ~2300 km^2 (Fig. 1, inset). Within a 4 km^2 area of each anchor station, three sampling transects comprising four sediment traps each were placed adjacent to tidal channels, with transect entry points chosen according to accessibility and stream order. Transects extended inland roughly normal to the channel bank, and the traps were spaced at 50–100 m intervals with the first trap site of each transect located ~50 m from the channel margin, away from prograding or retreating creek banks (Fig. 3). The setting for individual trap sites ranged from unvegetated or sparsely vegetated upper mudflats fringed with mangrove trees to areas with dense tree cover and extensive pneumatophores and undergrowth. Descriptions of each site can be found in supplementary Table 1. The most common mangrove species in the study areas are *Avicennia* sp. with thin, needle-like pneumatophores, and *Heritiera fomes*, which has pneumatophores ≤15 cm in diameter; grasses and reeds are typically absent. The sampling strategy was designed to capture the range of variability in vegetation, tidal inundation and geomorphology in the Sundarbans; however, local hydrodynamics were not measured at the 48 sampling sites.

Three different trap designs were chosen based on reviews of riparian sediment sampling methods tested by Steiger et al. (2003),

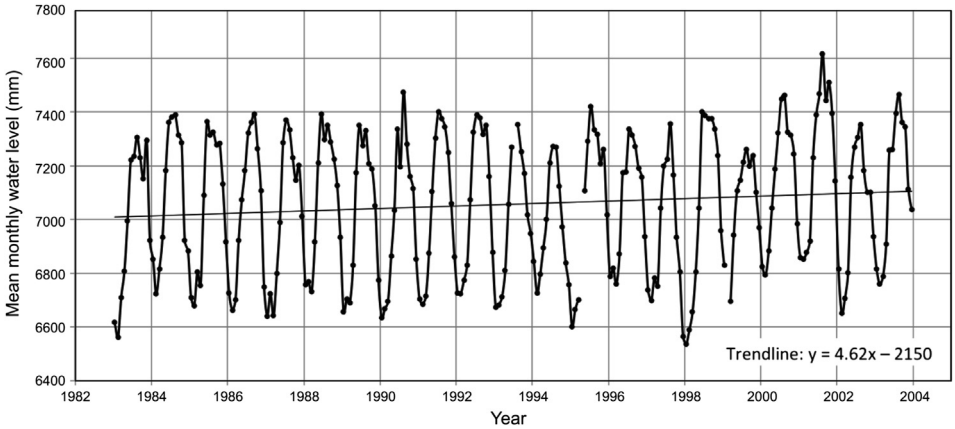

Fig. 2. Mean-monthly tide gauge data at the coast (Hiron Point; location in Fig. 1) showing 60–80 cm difference between summer and winter water levels; increase in summer reflects seasonal coastal set up, (source: PSMSL). The 24 year trend in relative sea level rise is ~0.5 cm yr^{-1}.

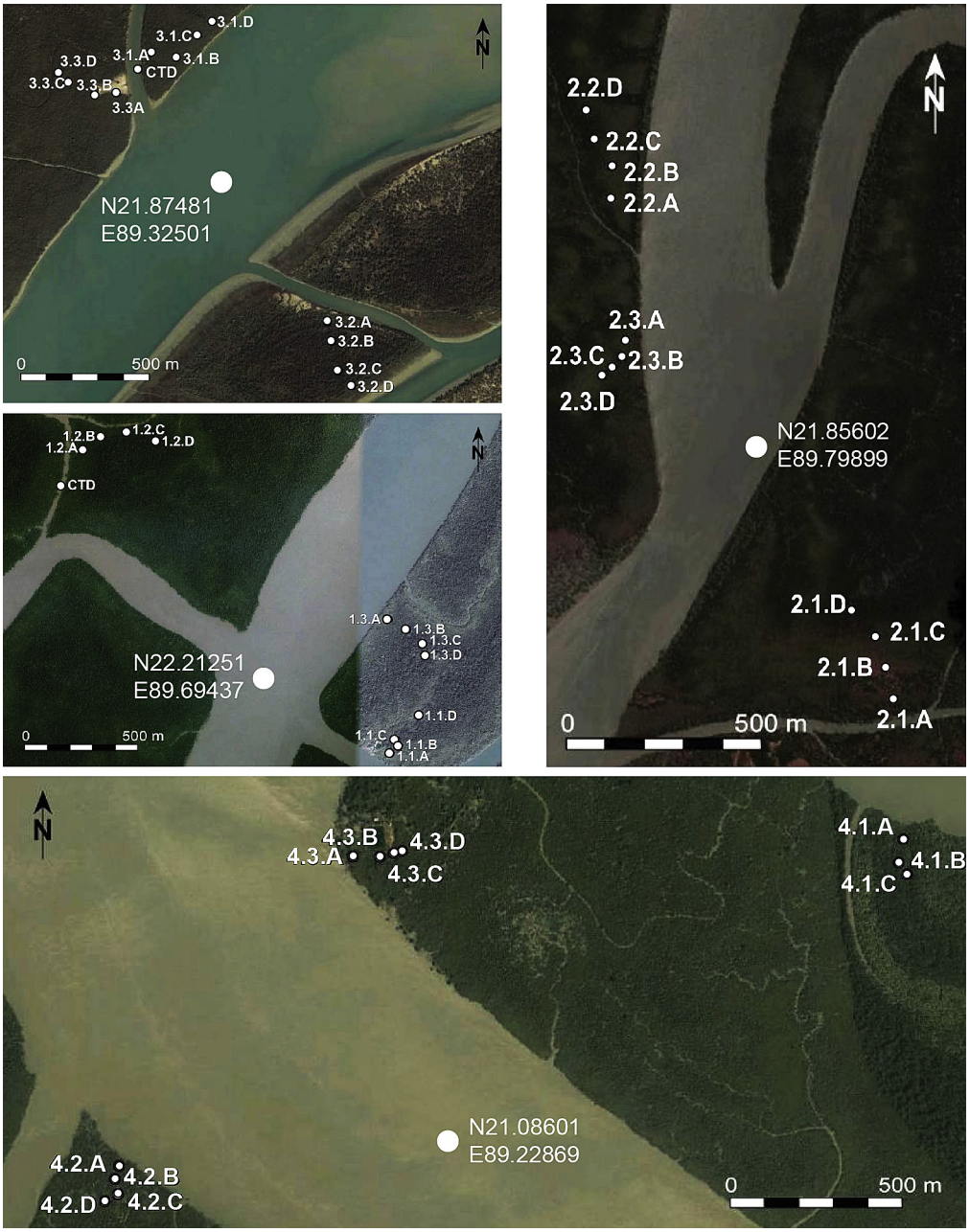

Fig. 3. Arrangement of trap sites. Anchor stations appear clockwise from top left: western coastal (station 3); eastern coastal (station 2); western inland (station 4), and eastern inland (station 1). Latitude and longitude indicate general location of anchor stations.

including: (1) 30 cm long × 5 cm diameter PVC pipes buried with 1 cm exposed above the forest platform; (2) 100 cm^2 artificial turf secured to the forest platform with 10 cm steel pins; and (3) 100 cm^2 ceramic tiles. In addition, a 2–3 mm-thick layer of brick dust was distributed on the ground surface adjacent to the traps (Fig. 4A). Brick dust was used to provide a qualitative indication of flow direction, depth of burial, and bioturbation. Traps were deployed over one monsoon flood season, totaling ~13 spring-neap tidal cycles from March to October. Samples were also collected in October from the upper 1 cm of sediment in adjacent tidal creek beds using Nalgene sample cups. No major storms occurred during the eight months the traps were in place.

All trap samples were retrieved in October 2008 following cessation of monsoon floodwaters, revealing that all were covered by sediment deposited over the eight-month deployment (Fig. 4B). In some locations, at least one of the sediment traps was missing or had been repositioned, most likely due to manipulation by faunal forest inhabitants. Shallow trenches were also dug at each site to expose the buried brick dust for measuring sediment thickness and recording qualitative observations of bioturbation and transport energy as indicated by dust dispersal. In the lab, sediment collected from the tiles and turf were homogenized, dried at 60 °C, and weighed for total mass accumulation. Radionuclide measurements on dried samples were started within two weeks of collection due to the short half-life of ^{7}Be. Dried aliquots of ~20 g of sediment were also combusted at 450 °C for ~6 h to determine the ashed weight of organic content. Grain size distributions were measured using a Malvern Mastersizer laser particle size analyzer.

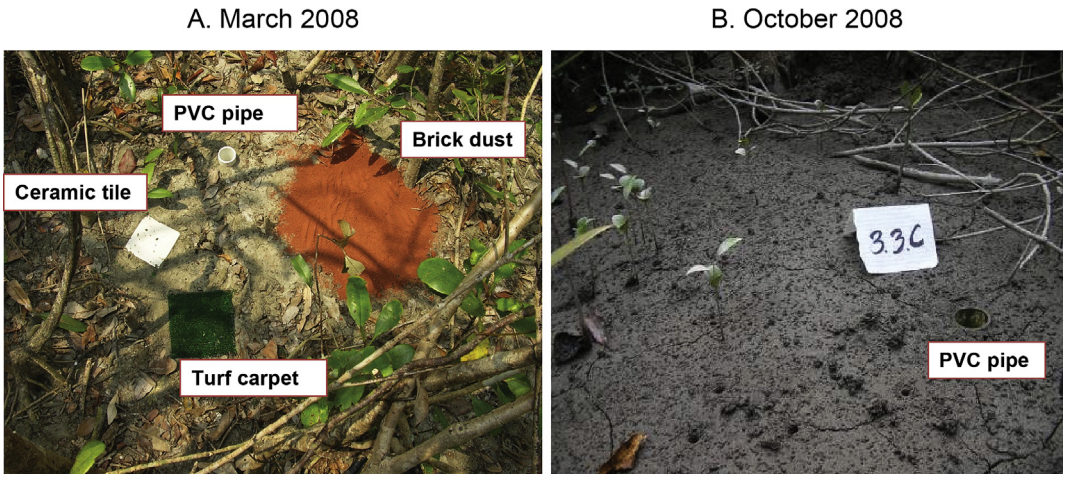

Fig. 4. Example of sediment trap site, A) pre- and B) post-monsoon. A. Typical trap array: PVC pipes captured gross sedimentation, turfs and tile captured net sediment accumulation and brick dust provided qualitative information regarding bioturbation and energy of the depositional environment. B. Example of trap site following monsoon flooding. Most trap sites were completely covered by sediment.

In addition to sediments collected from the delta plain and tidal creeks, suspended sediment was collected during peak monsoon flooding in August 2006 from water samples taken at nine inland river locations, including sites along the three main rivers (Ganges, Brahmaputra and Meghna), four distributaries, and two tributary channels. Suspended sediment samples were also collected from a tidal channel ~30 km east of the study area, and 5 km offshore. All suspended sediments were analyzed for grain size and radionuclide activities.

3.2. Radioisotopes

For the surface samples, 50–150 g of dried ground sediment was analyzed for ~24 h using two Ortec 125-mm^2 planar germanium gamma detectors. Detectors were calibrated using a custom mixed-gamma source and IAEA-375 soil standard. For the suspended sediment samples, the gamma decay spectra were measured on 3–6 g of dried sediment using a Canberra 16 mm-diameter germanium well detector at East Carolina University. Activities of ^{7}Be ($t_{1/2} = 53.3$ days; 477.7 KeV), ^{210}Pb ($t_{1/2} = 22.3$ years; 46.5 KeV), ^{234}Th ($t_{1/2} = 24.1$ days; 63.3 KeV) and ^{137}Cs ($t_{1/2} = 30.1$ years; 661 KeV) were recorded for all samples. Excess ^{210}Pb was also calculated by subtracting its in-situ supported level measured via ^{214}Pb and ^{214}Bi parents (295 and 352 KeV, and 609 KeV photopeaks, respectively) (Baskaran and Santschi, 1993; Matisoff et al., 2005). Activity values for all nuclides, especially short-lived ^{7}Be and ^{234}Th, were decay-corrected for loss from the time of sample collection to counting. Although activities of $^{234}Th_{xs}$ and ^{137}Cs were measured, activity values for ^{137}Cs were below detection for most samples and for all samples for $^{234}Th_{xs}$. The very low ^{137}Cs activities are consistent with previous results from the G–B tidal delta plain (Allison and Kepple, 2001).

The particle-surface reactivity, continuous atmospheric production and delivery, and relatively short half-lives of ^{7}Be and ^{210}Pb make them useful tracers of sediment movement across the land-sea boundary (Wang and Cornett, 1993; Bonniwell et al., 1999). Beryllium-7 is a naturally occurring cosmogenic fallout radionuclide produced continually in the atmosphere by the spallation of nitrogen and oxygen atoms. Beryllium-7 adsorbs to aerosols in the troposphere and is removed to the Earth's surface through wet and dry deposition (Turekian et al., 1983; Feng et al., 1999). Once delivered to the land surface, ^{7}Be ($K_d = 10^4$–10^6) rapidly attaches to soil particles and sediment, which may then be eroded and washed into a stream network (Hawley et al., 1986; Wallbrink and Murray, 1996). The primary source of ^{7}Be to sediments and the water column can be direct input from the atmosphere in some small watersheds (Olsen et al., 1986; Baskaran and Santschi, 1993). However, when the ratio of drainage area to estuarine surface area is high, such as it is in the G–B system (1.6×10^6 km^2 vs. $\sim 0.02 \times 10^6$ km^2), the input of ^{7}Be to the estuary is dominated by fluvial inputs sourced from the watershed (Baskaran et al., 1997; Sommerfield et al., 1999). In this study, ^{7}Be was used to determine the relative contribution of recently eroded (i.e. ≤6 months) river-sourced sediment deposited on the delta plain and tidal creek beds during the monsoon flood pulse. To increase the signal-to-noise ratio and account for minor additions of ^{7}Be from atmospheric fallout, we use a lower detection limit 0.2 dpm g^{-1} as a cutoff for measurable levels of ^{7}Be.

Like ^{7}Be, atmospherically produced $^{210}Pb_{xs}$ sorbs to terrestrial sediment in fluvial catchments and may be eroded and washed into channels, directly transported through the fluvial system, and eventually deposited on lower delta plains, estuaries, or continental shelves. Because of its 22.3-year half life ^{210}Pb geochronology may be used to investigate decadal-scale sedimentation rates and, when compared to ^{7}Be activities, provides information about the relative timing and input of sediment along the river-to-marine sediment transport pathway (Baskaran, 1995; Saari et al., 2010; Aalto and Nittrouer, 2012). The $^{7}Be/^{210}Pb_{xs}$ activity ratio typically varies much less along this transport path than the activities of the individual nuclides; therefore, changes in the ratio can reflect the time since the sediment was tagged with either nuclide, and may also indicate the degree of mixing of suspended sediment eroded from the floodplain surface (^{7}Be-enriched) with older (^{7}Be-deficient) sediment (Olsen et al., 1989; Matisoff et al., 2005).

4. Results

4.1. Sedimentation

Forty-seven of the 48 sample sites had recoverable sediment traps, and despite the variety of vegetation, topography and sampling locations on the tidal delta plain, all sites received measurable deposition in the 8-month sampling period (Fig. 5). Of the three traps types that were deployed, tiles proved to be the most effective for determining net sediment accumulation. All but eight tiles were recovered, and the turf samplers were used at sites with missing tiles. The brick dust layer was preserved at all locations and was

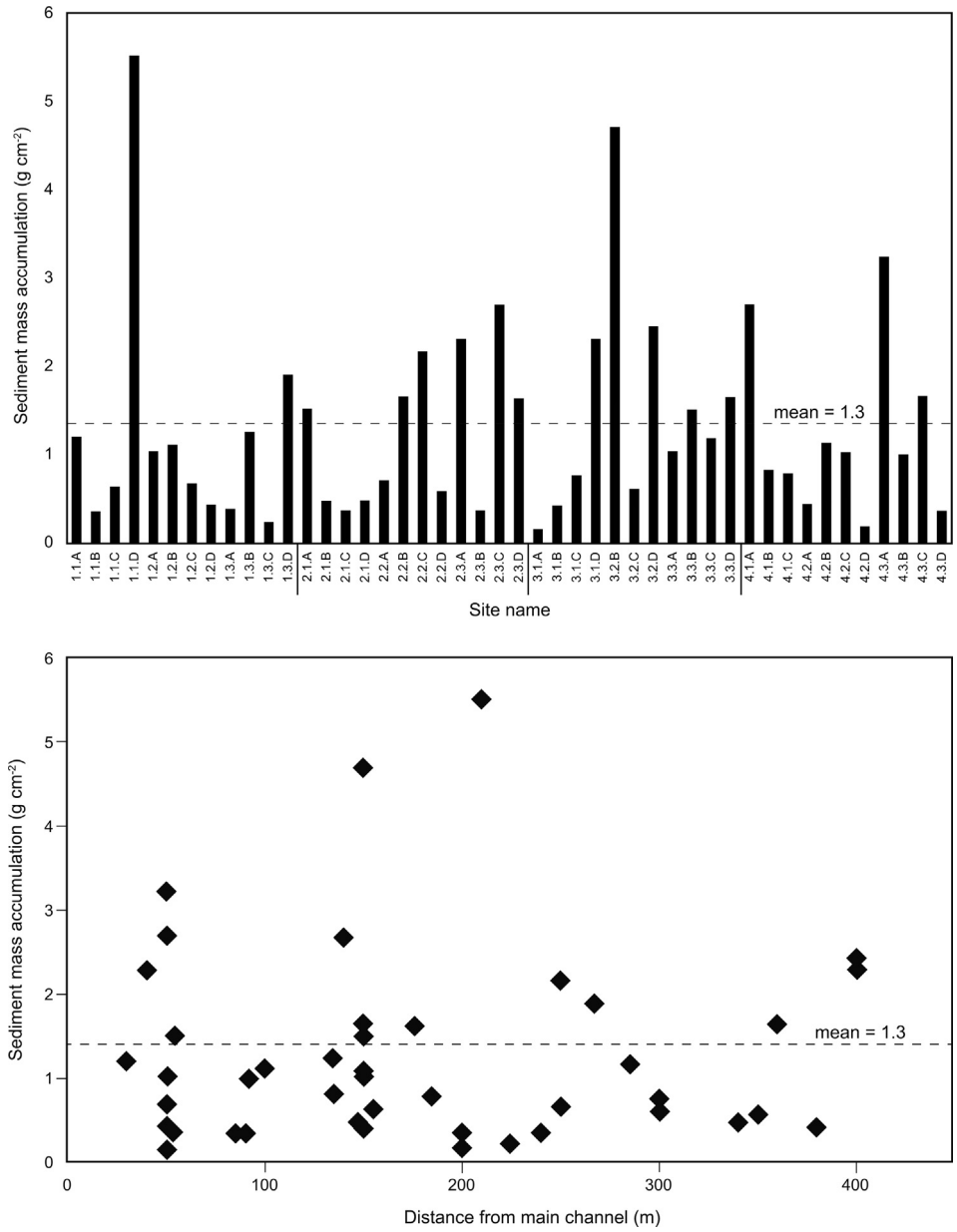

Fig. 5. Sediment mass accumulation trends for all sites where traps were recovered. Top panel shows mass accumulation values for each site; all trap sites received sediment during the 2008 monsoon season. Bottom panel shows mass accumulation versus distance from main channels, illustrating the variability in along-transect deposition trends.

useful in demonstrating that no significant erosion or scour had occurred during the deployment. Vertical mixing of the brick-dust layer showed minimal bioturbation during the sampling interval, with downward mixing extending locally <3 cm below the brick dust layer. Among the 29 PVC pipes recovered, sediments infilled 3–57% of the volume (mean = 20%) and were texturally homogenous with no apparent bedding and little particulate organic matter. Vegetation type and density was documented and correlated to observed accretion rates at each site, with no discernable trends. Among the physical characteristics measured for the deposited sediments, the most notable result is that mean values for all measured attributes are very similar between stations (Table 1). Complete sedimentological and radionuclide results are shown for each trap site in supplementary Table 1.

Mass accumulation values across the study area range from 0.1 to 5.5 g cm^{-2} with an average of 1.3 ± 1.1 g cm^{-2}. The dataset is normally distributed and reveals similar maximum/minimum values among the anchor stations (Table 1). Two main trends in sedimentation emerge at the transect scale. First, accumulation values in half of the transects decreased with distance from the channel before increasing again at terminal sites. In these transects, terminal trap sites (i.e. those positioned farthest away from main deployment channels) were located ≤5 m from smaller order inland creeks. Another 40% of transects show an overall mean decrease of 69% in sediment accumulation from channel edges to terminal sites. The remaining 10% of transects contained relatively consistent values along their entire length. Since all trap sites in the Sundarbans received sediment, such local-scale differences indicate (1) smaller order streams are carrying sediment to the interior of tidal islands; flooding of these small internal creeks results in deposition near the creek edges, producing the observed increase in sedimentation at terminal sites, and (2) where transects are not

Table 1
Summary of results from delta plain, creek bed and 2006 floodpulse sediments (*std dev* = standard deviation).

	E. Inland	E. Coastal	W. Inland	W. Coastal	All delta plain stations	Creek bed	Flood pulse
Net mass accumulation (g cm^{-2})							
Max	5.5	2.7	3.2	4.7		NA	NA
Min	0.2	0.4	0.2	0.1		NA	NA
Mean ± std dev	1.2 ± 1.4	1.2 ± 0.9	1.2 ± 1.0	1.5 ± 1.3	1.3 ± 1.1	NA	NA
Gross mass accumulation (g cm^{-2})							
Max	22.1	9.1	19.5	15.0		NA	NA
Min	2.6	1.3	2.6	5.2		NA	NA
Mean ± std dev	9.2 ± 6.6	5.5 ± 2.9	9.1 ± 5.3	9.6 ± 3.8	8.4 ± 1.9	NA	NA
Accretion rate (cm yr^{-1})							
Max	4.2	2.1	2.5	3.6		NA	NA
Min	0.2	0.3	0.1	0.1		NA	NA
Mean ± std dev	0.9 ± 1.1	1.0 ± 0.7	0.9 ± 0.7	1.2 ± 1.0	1.0 ± 0.9	NA	NA
Grain size (μm)							
Max	42.2	41.4	30.4	48.5		45.6	27.6
Min	18.3	24.2	16.3	16.6		22.7	12.3
Mean ± std dev	28.6 ± 6.4	30.3 ± 5.2	23.5 ± 4.7	28.5 ± 10.1	27.7 ± 7.2	34.4 ± 8.4	19.1 ± 5.9
Organic content (%)							
Max	2.9	3.8	2.9	3.1		NA	NA
Min	0.6	0.7	0.6	0.4		NA	NA
Mean	1.4 ± 0.9	1.4 ± 0.8	1.3 ± 0.7	1.6 ± 0.9	1.4 ± 0.8	NA	NA
^{7}Be activity (dpm g^{-1})							
Max	1.9	1.4	1.3	1.0		0.9	1.4
Min	0.2	0.2	0.2	0.2		0.4	0.0
Mean ± std dev	0.6 ± 0.6	0.8 ± 0.4	0.8 ± 0.4	0.5 ± 0.3	0.7 ± 0.4	0.5 ± 0.3	0.7 ± 0.3
^{7}Be inventory (dpm g^{-1} cm^{-2})							
Max	0.9	1.9	1.3	1.6		NA	NA
Min	0.0	0.2	0.0	0.2		NA	NA
Mean ± std dev	0.3 ± 0.3	0.5 ± 0.6	0.6 ± 1.4	0.4 ± 0.4	0.5 ± 0.7	NA	NA
$^{210}Pb_{xs}$ activity (dpm g^{-1})							
Max	3.6	3.4	5.1	3.6		1.9	2.0
Min	0.2	0.4	0.6	0.5		0.5	0.3
Mean ± std dev	1.6 ± 1.2	1.6 ± 1.1	2.1 ± 1.2	1.5 ± 0.9	1.7 ± 1.1	1.7 ± 1.1	1.3 ± 0.6
$^{210}Pb_{xs}$ inventory (dpm g^{-1} cm^{-2})							
Max	2.3	3.9	3.7	4.3		NA	NA
Min	0.1	0.6	0.5	0.5		NA	NA
Mean ± std dev	1.2 ± 0.6	1.3 ± 0.9	1.8 ± 1.0	1.6 ± 1.0	1.4 ± 0.9	NA	NA
^{7}Be:$^{210}Pb_{xs}$ activity ratio							
Max	0.50	1.10	0.50	0.50		1.04	NA
Min	0.10	0.20	0.20	0.10		0.21	NA
Mean ± std dev	0.29 ± 0.15	0.48 ± 0.28	0.36 ± 0.11	0.33 ± 0.11	0.36 ± 0.18	0.42 ± 0.35	0.54 ± 0.45

bound on the distal end by small creeks, deposition follows the expected pattern for overland flooding with decreasing deposition away from channel edges. Local variations in microtopography or vegetation density may also produce hydrodynamic conditions that influence mass accumulation at individual trap sites, though these attributes were not measured in this study. Regardless of local differences, sediment accumulation values are generally similar at all four stations. This suggests that larger-scale sediment distribution processes are operating at a similar magnitude in all parts of the lower delta plain, despite being geographically widespread and far from the river mouth. The normal distribution and similar range of values between each anchor station demonstrates that the dataset captures the extent of local to regional variability in accumulation and is not biased by any significant outliers. This is further supported by the observation that mean mass accumulation values and their standard deviation are nearly identical among the four anchor stations (1.2–1.5 ± 0.9–1.5 g cm^{-2}; Table 1). The relatively high standard deviations among these sites reflects the expected local heterogeneity in short-term sedimentation patterns, but the similarity of the integrated means indicate a regionally coherent pattern of deposition.

The limited difference in results among the anchor stations indicates that sites located up to 50 km inland received as much overall sediment as those located on the coast. Similarly, sites in the western Sundarbans received slightly more sediment on average than those in the east (1.4 ± 1.2 vs. 1.2 ± 0.4 g cm^{-2}) despite being >50 km further from the G–B river mouth. These results suggest that there is not a rapid decay of suspended sediment concentration within 150 km of the rivermouth, and also that the SoNG canyon is not a significant barrier to nearshore sediment transport along the inner shelf. The modestly higher sedimentation in the more distal western Sundarbans may be explained by its relatively lower elevation compared with the eastern Sundarbans (e.g. Ellison et al., 2000), which supports an increased depth, duration, and frequency of flooding by sediment-laden tidal waters (French and Spencer, 1993; Reed, 2002; Adame et al., 2010).

Compared with 'net' deposition measured from the tiles, sedimentation within the PVC pipes can be a good indicator of 'gross' or 'potential' accretion, since the tubes are effective traps that retain any sediments accumulating within them. Thus, mass accretion in the PVC pipes should be proportional to the integrated mass of suspended sediment that each site is exposed to during tidal inundation. Results overall show wide scatter and generally poor correlation with surface accretion values, but on average the PVC pipes trapped 7.5 times more sediment than tiles and turf at the same locations (Table 1). However, spatial differences show that PVC pipes from the western stations (9.3 ± 4.5 g cm^{-2}) trapped ~9 times more sediment than local surface deposition, whereas the eastern PVC pipes (7.5 ± 5.4 g cm^{-2}) only trapped ~5 times more than surface accretion. This finding is consistent with the interpretation that

slightly higher surface accretion values observed for western sites are a consequence of that area's lower elevation, and thus its greater and more frequent inundation by the tides.

4.2. Sediment attributes

4.2.1. Grain size

Considering the size and complexity of the Sundarbans, overall volume weighted grain size averages for delta plain and creek bed sediments fall within a narrow range of silt-dominated values from 16.3 to 48.5 μm (Table 1; supplementary Fig. 1). Newly deposited sediments consisted of 16 ± 4% clays (<4 μm), 76 ± 3% silts (4–63 μm) and 8 ± 4% sands (>63 μm). Western inland sites had the finest mean grain size (23.5 ± 4.7 μm) of the four study areas, compared with 28.5 ± 10.1 to 30.3 ± 5.2 μm for the other stations. Otherwise, the grain size variations among the sites and along transects revealed no discernable trends. Sediments collected from creek beds adjacent to the transects were also dominated by silts (volume weighted mean: 25.4–45.6 μm).

4.2.2. Organic content

Soil organic carbon measured through loss-on-ignition (LOI) ranges from 0.4 to 3.8% in the tidal delta plain, averaging 1.4 ± 0.8% in both the eastern and western Sundarbans (Table 1). While these values are comparable to previous measurements of soil organic content from the Sundarbans (1.7%), overall they are very low compared to the worldwide mean of 7.9% for estuarine tropical mangrove systems (Donato et al., 2011). Other alluvial-deltaic mangrove systems, such as the Mahakam (Indonesia) or Orinoco (Venezuela) deltas, have sediment organic contents of 7–24%, or up to 14 times that found in the Sundarbans (Vegas-Vilarrúbia et al., 2010; Donato et al., 2011). The lower G–B delta plain differs from these and other tropical delta systems in its very large sediment loading, which appears to maintain high sedimentation rates that dilute accumulated organics, as well as a higher, better-drained land surface suited to exporting surface organic matter (Lynch et al., 1989; Allison, 1998; Allison and Kepple, 2001). To assess whether the low LOI values are a function of dilution of organic material by the large siliciclastic input, mass accumulation was plotted against soil organic content. This exercise produced no obvious trends between sedimentation and soil organic content, indicating the low LOI values are not the result of dilution by rapid sedimentation, nor is there significant import of organic matter into the system by tides or coastal set-up. Rather, the low soil organic content of the Sundarbans points to rapid tidal export of locally produced organic matter to the coastal zone.

4.3. Radionuclide data

4.3.1. Beryllium-7

Sediments deposited during the 2008 monsoon season had detectable ^{7}Be at about ½ of the 48 sampling sites but often at relatively low activity levels, from the detection limit of 0.2 dpm g^{-1}–1.9 dpm g^{-1} (Table 1). Traps containing sediment with detectable ^{7}Be were equally distributed among the four sampling stations, and each transect included at least one site with detectable ^{7}Be. Additionally, ^{7}Be was present on sediment in 98% of traps at sites located at the end of transects. Because ^{7}Be is particle bound and preferentially sorbs to fine-grained sediments, ^{7}Be inventories can vary with grain size. To test for the influence of grain size, corrections were applied to radionuclide activities (e.g., Goodbred and Kuehl, 1998) but produced minimal difference in results due to the narrow range of grain sizes and homogeneity of sediment texture across the study area. Here we use the uncorrected data for inventory calculations to avoid the introduction of bias or additional error.

Total ^{7}Be inventories were calculated and plotted against sediment mass accumulation to distinguish whether the principal source of measured ^{7}Be was from direct atmospheric fallout or sorbed to suspended river sediment (Fig. 6A). Results show that inventories increase with accumulation, indicating that ^{7}Be is added with the input of new sediment. If ^{7}Be were principally atmospherically derived, increased sediment input would have no effect on inventory values. This suggests that ^{7}Be is primarily sourced from seasonal flood pulse sediments already tagged with ^{7}Be from the catchment. Further supporting this interpretation is the range of ^{7}Be activities (e.g. 0.4–0.9 dpm g^{-1}) on all but one of the creek bed samples, which were within the same range of activities on those from exposed delta plain sites (0.2–1.9 dpm g^{-1}), even though creek beds are only subaerially exposed at low tide or not at all. That is, ^{7}Be-tagged sediments accumulating in both tidal creeks and on the delta plain appear to be sourced from the monsoon flood discharge of the G–B River. This is further reflected in the similar ^{7}Be activities measured on suspended flood pulse sediments during 2006 peak discharge within the mainstem river and 5-km offshore of the coast (0.7 ± 0.3 dpm g^{-1}) compared with bed sediments from the tidal creeks (0.5 ± 0.3 dpm g^{-1}) and delta

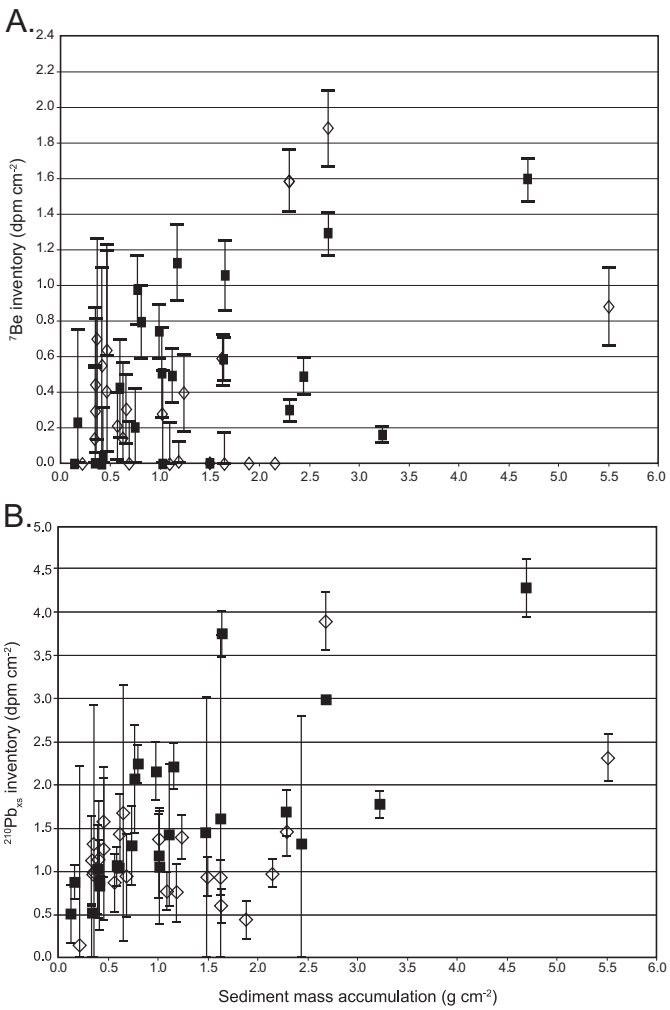

Fig. 6. Comparison of A. ^{7}Be and B. ^{210}Pb$_{xs}$ inventories to sediment mass accumulation in eastern (diamonds) and western (squares) showing overall increase in inventories with increasing sediment accumulation, suggesting these radionuclides are sourced from the terrestrial flood pulse, rather than from atmospheric fallout.

plain (0.7 ± 0.4 dpm g^{-1}) (Table 1). Although discharge and river dynamics may have differed between 2006 and 2008, the large catchment (1.6 × 10^6 km^2) serves as an effective buffer of high-frequency variability and yields a strongly averaged discharge signal at the rivermouth. Furthermore, the robust monsoon climate of the G–B catchment constrains interannual variability in discharge to ±20%, which should limit significant variation in nuclide activities between the two years (Jian et al., 2009). Of the suspended sediment samples measured in 2006, those from the Brahmaputra River and offshore were tagged with detectable ^{7}Be. The ^{7}Be activity on other suspended sediment samples, however, were at or below detection limits, suggesting that there is local dilution with ^{7}Be-deficient particles eroded from channel banks or resuspended from older bottom sediments (Matisoff et al., 2002, 2005). Nevertheless, these results indicate that the rivers are rapidly transporting and discharging to the inner shelf ^{7}Be-tagged sediment eroded from the surface of the G–B fluvial catchment. On the shelf, the river sediment plume is dispersed westward by prevailing currents, where it remains in suspension and available for transport onshore via tidal creeks and onto the delta plain (Kuehl et al., 1989; Barua et al., 1994).

4.3.2. Lead-210

Just as ^{7}Be is an effective tracer of suspended sediment dynamics on seasonal time scales, the 22.3-year half life of ^{210}Pb makes it useful for studying rates of erosion, transport and deposition on time scales of 100 years or less. Traditionally, ^{210}Pb geochronology has been applied to sediment cores collected in lacustrine, marine and floodplain settings to determine decadal-scale accretion rates (e.g. Wallbrink and Murray, 1993; He and Walling, 1996; Matisoff et al., 2002; Aalto and Nittrouer, 2012). In this study, $^{210}Pb_{xs}$ activities are evaluated to identify the potential sources of sediment seasonally accreting on the Sundarbans delta plain surface.

The mean $^{210}Pb_{xs}$ activities of sediment deposited during the 2008 monsoon range from 1.6 ± 1.1 to 1.8 ± 1.1 dpm g^{-1} (Table 1). These values are within the range of average $^{210}Pb_{xs}$ activities measured on suspended sediment from the 2006 peak discharge (0.7–1.9 dpm g^{-1}). Delta plain $^{210}Pb_{xs}$ activities are also similar to those measured on surface sediment (<10 cm) in the Brahmaputra floodplain and central G–B delta plain ~80 km northeast of the Sundarbans (1.5–2.1 dpm g^{-1}) (Goodbred and Kuehl, 1998). The consistency of $^{210}Pb_{xs}$ values throughout these geomorphically diverse settings of the delta suggests that: (1) the rivers deliver near-surface sediment eroded from catchment soils within the past ~100 yrs; (2) fluvial and marine transport processes effectively distribute sediment across large areas of the delta; and (3) most of the sediment accreted on the tidal delta plain during the 2008 monsoon flood was sourced from the catchment within the last century.

The positively correlated relationship between $^{210}Pb_{xs}$ inventories and sediment mass accumulation (Fig. 6B) indicates that the amount of $^{210}Pb_{xs}$ at trap sites increases with sediment input, indicating that the dominant source of $^{210}Pb_{xs}$ is sorbed to incoming sediments. Just as with ^{7}Be, localized atmospheric input of $^{210}Pb_{xs}$ would cause the inventory to vary independently of mass accumulation, and higher sedimentation would have no effect on total $^{210}Pb_{xs}$ inventory. These results, for both $^{210}Pb_{xs}$ and ^{7}Be, support a fluvial sediment source for these radionuclides rather than direct atmospheric fallout. Likewise, the mean $^{210}Pb_{xs}$ activity (1.7 ± 1.1 dpm g^{-1}) of surface creek-bed sediments is identical to that for surface sediments on the tidal delta plain (1.7 ± 1.1 dpm g^{-1}), suggesting a similar origin for sediments deposited in both settings. This also indicates that there is minimal dilution of the $^{210}Pb_{xs}$ signal in tidal creeks by older (>100 yrs) particles, which would effectively lower mean creek bed $^{210}Pb_{xs}$ activities relative to delta plain activities.

4.3.3. ^{7}Be/$^{210}Pb_{xs}$ activity ratio

Because ^{7}Be and $^{210}Pb_{xs}$ have different half lives and fluxes to Earth's surface, their activity ratio is useful for studying sediment transport in estuarine settings. Once atmospheric ^{7}Be and ^{210}Pb are sorbed to sediment, their activity ratio changes through the more rapid decay of ^{7}Be and by dilution with particles deficient in either radionuclide, including dilution by older reworked fluid muds (Koch et al., 1996). Although the ^{7}Be/$^{210}Pb_{xs}$ activity ratio increases slightly from 0.2 in suspended tidal creek sediments to 0.5 in surface sediment collected from creek beds, the overall ratio decreases from 0.6 in the G–B river to 0.4 on the delta plain (Fig. 7). This indicates that ^{7}Be-tagged sediments are diluted with ~33% ^{7}Be-deficient sediments along the river-to-delta plain transport path. The activity ratio is lowest on suspended tidal channel sediments, which is also where the lowest activity of ^{7}Be is recorded along the transport pathway, indicating that some ^{7}Be-deficient sediments are resuspended within tidal creeks during transport.

5. Discussion

5.1. Sources of tidal delta-plain sediments

The results presented here indicate that the 'abandoned' G–B tidal delta is accreting from a mix of sediments tagged with ^{7}Be in the river catchment and dispersed from the river mouth to the Bengal shelf, plus older ^{7}Be-deficient sediment reworked from the shelf or tidal channels. Taken together, these findings confirm that there is a direct link between the lower G–B delta plain and the active river mouth, despite the large distance (>100 km) and limited connectivity between them. Distinguishing the contribution of each sediment source to delta plain accretion clarifies the processes that are most important for maintaining the G–B delta's positive elevation and is critical for informing effective management practices of this and other deltaic coastlines threatened by sea level rise. To that end, it is instructive to estimate the amount of 2008 flood-pulse sediment that contributed to the total mass deposited at each delta plain site during the trap deployment. A estimate of this flood pulse contribution can be made by dividing

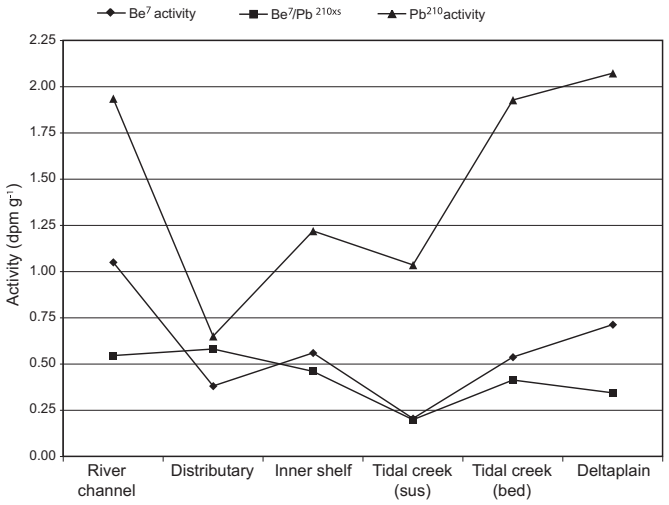

Fig. 7. Average ^{7}Be and $^{210}Pb_{xs}$ activities and ^{7}Be:$^{210}Pb_{xs}$ ratios from river source to delta plain sink. Individual nuclide activities follow the same relative trends, whereas the ^{7}Be:$^{210}Pb_{xs}$ activity ratio decreases along the source-to-sink path reflecting dilution/decay of ^{7}Be, or enhancement of $^{210}Pb_{xs}$.

mean ^{7}Be activities of delta plain sediments at each site by the average detectable ^{7}Be activity measured on suspended sediments from the river during peak monsoon flooding (1.05 ± 0.3 dpm g^{-1}; Table 2).

Results indicate that ^{7}Be-tagged sediment delivered by the G–B river within the 6 months prior to sampling (i.e. May–October, 2008) comprised a mean of 63% of the sediment accumulating on the delta plain during this time. Despite being the farthest away and least likely to receive direct riverine sediment input, sediments deposited at the western inland sites comprised 75% of annual flood pulse sediments, which is equivalent to the amount received at eastern coastal sites located closer to the river mouth. These overall findings emphasize the effectiveness of tides and monsoon set-up in transporting sediment to inland sites far from the coast and from the river mouth. In sum, more than half of the sediment accretion that is sustaining the Sundarbans tidal delta against rising relative sea level appears to be sourced directly from the mouth of the G–B River during high discharge.

The remaining sediments deposited on the delta plain during deployment were ^{7}Be-deficient sediments that originated from several possible sources. One source may be muds seasonally stored in shallow waters (<20 m) on the vast (~10^{5} km^{2}) inner shelf. Based on the observations of Kuehl et al. (1989), much of the inner shelf is blanketed by a discontinuous mud drape from 0.05 to 1 m thick that is stored seasonally before being reworked onshore or into deeper water at the clinothem foresets or canyon head. Taking a conservative estimate of a 0.05 m-thick ephemeral mud deposit integrated over half of the inner shelf (~5000 km^{2}), such a mud drape would represent a seasonal storage of at least 32.5 × 10^{6} metric tons of sediment, which is equivalent to ~5% of the annual sediment load reaching the coast. These ^{7}Be-tagged sediments discharged at the river mouth mix with ^{7}Be-deficient sediments on the inner-shelf, lowering the mean ^{7}Be activity of suspended sediments delivered to the delta plain. Another likely source of ^{7}Be-deficient sediments are those temporarily stored within the extensive tidal channel network of the Sundarbans, evidenced by the loosely consolidated, slumping sediments that line the banks of many smaller creeks.

5.2. Accretion rates vs. relative sea level rise

In order to place the observed mass accumulation values in context of delta stability and sea level rise, accretion is compared to tide gauge data from the Bengal coast. Mass sediment accumulation is converted to a unit length by dividing by dry bulk density, here using a mean value of 1.3 g cm^{-3} (Allison and Kepple, 2001). The resulting mean accretion rate for all sites in the Sundarbans is 1.0 ± 0.9 cm yr^{-1} (Table 1). This is consistent with accumulation measured in other river-dominated mangrove systems with large sediment supplies (e.g. Gulf of Papua [Walsh and Nittrouer, 2004]). Relative sea level rise (RSLR) data averaged from three tide gauge stations across the G–B delta front (Fig. 1) cover at least one lunar nodal cycle with differing rates of RSLR. The two 24-yr tide-gauge records near closest to the study area provide 24 years of data and yield local rates of RSLR of 0.5 cm yr^{-1} at Hiron Point and 1.5 cm yr^{-1} at Khepupara. A third tide gauge (Hatia), ~140 km to the east of the study area in the river mouth estuary, gives a local rate of 0.5 cm yr^{-1} over a 21-yr period (PSMSL, 2002, 2005). The origin of the high rate recorded at Khepupara near our eastern study sites is not known and may represent a local maximum related to subsidence, compaction, or an issue with the gauge installation. However, given uncertainties regarding these variations, we take 1.5 cm yr^{-1} and 0.5 cm yr^{-1} as maximum and minimum rates for local RSLR in the study area and 1.0 cm yr^{-1} as the average. This is equivalent to the maximum centennial-scale RSLR of 0.9 ± 3.3 cm yr^{-1} estimated for the Sundarbans coast based on subsidence rates obtained through the dating of buried salt kilns and mangrove root horizons (Hanebuth et al., 2013).

By comparison, the vertical sedimentation rate of 1.0 ± 0.9 cm yr^{-1} on the tidal delta plain is generally in equilibrium with the ~1.0 cm yr^{-1} average rates of RSLR at the Bengal coast. However, spatial variations in annual deposition could result in a non-uniform response of the lower delta plain to increased sea level. For instance, in the parts of the delta where sedimentation is highest near the edges of tidal creeks relative to interior sites (~50% of all transects), the fringe of tidal islands may keep pace with sea level rise due to enhanced sedimentation while the interior may become increasingly water logged and slow draining. The opposite may be true, however, for the frontal edge of islands facing the Bay of Bengal where an estimated net land loss of 0.7% between 1986 and 2007 was documented from time-series analyses of Landsat images (Shearman et al., 2013). Regardless, there is no evidence for degradation of interior areas of the Sundarbans to date. The large standard deviation and normal distribution of sedimentation rates recorded from all parts of the Sundarbans suggests that these local variabilities likely average out over decadal time scales. The rapid colonization by mangroves and stabilization of newly formed islands at the mouth of tidal estuaries along the delta front also offsets erosion. This is supported by comparisons of satellite data with historical shoreline survey charts that indicate that despite minor erosion along its seaward edges, the overall morphology of the tidal delta plain has remained largely consistent for at least the past 200 years (Allison, 1998).

Table 2
Percent of delta plain sediments tagged and eroded from catchment surface within ≤6 months.

	Floodpulse	E inland	E coastal	W coastal	W inland
Mean ^{7}Be activity	1.05	0.6	0.8	0.5	0.8
Standard deviation	±0.5	±0.6	±0.4	±0.3	±0.4
Percent of total		55%	77%	45%	76%
Mass accumulation (g cm^{-2})		1.2	1.2	1.5	1.2
Standard deviation		±1.4	±0.9	±1.3	±1.0
Overall mean	63%				
Eastern stations (mean)	69%				
Western stations (mean)	60%				
Inland stations (mean)	69%				
Coastal stations (mean)	61%				

5.3. Sediment budget

Sediment budget calculations identify sediment sources and sinks in a delta system and allow predictions of how changes to the rate of sediment import or export might be reflected in a delta's construction or deconstruction. The sediment budget for the Ganges–Brahmaputra delta system has been fairly well constrained for the river floodplain and subaqueous delta. Through the use of geochronological, seismic and stratigraphic analyses, it has been estimated that of the ~10^{9} tons of sediment annually discharged by the Ganges–Brahmaputra River, ~30% is sequestered in the floodplain and 40% is deposited on the rapidly prograding marine clinothem (Eysink, 1983; Kuehl et al., 1997; Goodbred and Kuehl, 1998, 1999). How the remaining 30% is partitioned between the Swatch of No Ground canyon and the lower delta can now be better defined using the mass accumulation results presented here.

The sediment budget for the lower delta plain was determined by multiplying mass accumulation by area. The total area of the Sundarbans in Bangladesh is ~6400 km^2, with another ~3600 km^2 in India, for a total area of ~10,000 km^2. A two-color Landsat classification analysis was conducted on an image taken at mid-tide 2 days before maximum spring tide during the dry season (November 2006) to determine the approximate land to water ratio in the Bangladeshi Sundarbans. Based on this analysis, 73 ± 3% of the region is forested intertidal delta plain, which is equivalent to ~4800 km^2. Since accumulation results appear to have captured the range of variability in deposition and traps were placed in a variety of vegetative and morphological settings, we take 1.3 ± 1.1 g cm^{-2} as the overall mean accumulation across the tidal delta plain. If this value is extended to the 4800 km^2 intertidal area estimated for the Bangladeshi Sundarbans, then ~62 × 10^6 t of sediment was deposited on the tidal delta plain during the 2008 monsoon season. This accounts for 6.2% of total annual G–B discharge and ~9% of the 700 × 10^6 t estimated to reach the coast during the monsoon (Table 3).

Although the above calculation provides a reasonable approximation of seasonal sedimentation for the Bangladeshi Sundarbans, it is likely a minimum for the total accumulated in the mangrove coastal plain of the Ganges–Brahmaputra delta. The actual total deposited on the lower delta could be higher for several reasons. First, this budget estimate is limited to the forested delta plain and does not include sediment storage in the extensive tidal channels. Second, deposition in the ~3600 km^2 of the Indian Sundarbans would contribute considerably to the total mass accumulation on the lower delta, though direct measurements of modern sedimentation have not been recorded here. Given the uncertainty regarding G–B sediment input west of the canyon and the distance between the G–B river mouth and the western shelf (>200 km), accretion rates in the Indian Sundarbans could be between 20 and 50% of that in the Bangladeshi Sundarbans, contributing an additional 13–32 × 10^6 t y^{-1} of sediment storage. Together, the total storage across the whole of the Sundarbans could range from 77 to 96 × 10^6 t y^{-1}, representing 8–10% of the total annual sediment load of the G–B river system.

The 8-month length of the sampling period could also make the observed mass accumulation values a minimum annual rate. For example, even though sediment discharge is an order of magnitude less in the dry season, reworking of sediments by tropical storms and tidal currents may nevertheless contribute to deposition outside of the high-discharge monsoon season (Barua, 1990). Dry season sedimentation could account for an additional 2–3 × 10^6 t yr^{-1} considering reduced overall discharge and relaxation of onshore winds that are otherwise important for sediment delivery to inland sites during summer months. Regardless, the minimum estimated sedimentation of 62 × 10^6 t yr^{-1} calculated for the Bangladeshi Sundarbans is 40% greater than the previous budget estimate of 37 × 10^6 t yr^{-1} for the combined Indian and Bangladeshi Sundarbans determined through the use of radiocarbon- and ^{137}Cs-dated sediment cores (Allison and Kepple, 2001). If sedimentation in the Indian Sundarbans and dry-season deposition are included in the current estimate, then the total sediment deposited on the combined Sundarbans could be as much as 100 × 10^6 t yr^{-1}.

Finally, interannual variability in monsoon precipitation may impact water and sediment discharge at the river mouth, thus altering the amount of flood pulse sediment available on the shelf for dispersal to the tidal delta plain. Corroborated satellite altimetry and in-situ water level measurements confirm that precipitation and river discharge in the Brahmaputra River basin was anomalously high in 2008, although Ganges discharge was below average that year (Papa et al., 2010, 2012). The combined values yield a discharge anomaly that was 19% above the 15-year mean (1993–2008) in 2008, which is only the third highest discharge during that time. Nevertheless, since the ^{7}Be results of this study indicate that over half of the sediments deposited on the tidal delta plain in 2008 were sourced from the flood pulse, our sedimentation results could represent above average accumulation rates. By comparison, though, our mean annual accretion rate of 1.0 cm^2 yr^{-1} is the essentially the same as that determined for the past 50 years using ^{137}Cs geochronology (1.1 cm^2 yr^{-1}; Allison and Kepple, 2001).

Revisiting earlier sediment budgets for the modern dispersal system: ~300 million tons of fluvial sediment annually delivered to the Bengal basin is stored on the floodplain, and the remaining ~750 million tons is discharged at the river mouth. On the shelf, the fluvial sediment load is partitioned between the topsets and foresets of the subaqueous delta (~400 million tons), and until now, the remaining 350 million tons was thought to bypass the shelf to the deep sea via the canyon. The results of this study indicate the Sundarbans tidal delta plain is also a significant sink for sediment discharged at the coast, potentially storing up to 100 million tons of the annual fluvial sediment load, or 10% of the total annual G–B river discharge. Although the Sundarbans is a small area when compared to the world's drainage basins (0.005%), it stores >0.6% of the sediment estimated to be discharging from rivers to the modern coastal ocean (Syvitski and Kettner, 2011; Table 3).

Table 3
Sundarbans sediment budget.

	Land area (km^2)	Storage (10^6 t y^{-1})	% Of total G–B Q_s*	% Of global Q_s pre-Anthropocene†	% Of global Q_s modern‡
Bangladesh	4800	62.4	6.2	0.4	0.5
India	3000	13–32	1.3–3.2	0.09–0.2	0.1–0.25
Total	8000	77.4–96.4	8–10	0.5–0.6	0.6–0.7

* Average 10^9 t yr^{-1} (Milliman and Syvitski, 1992).
† Estimated as 15.1 × 10^9 t yr^{-1} (Syvitski and Kettner, 2011).
‡ Estimated as 12.8 × 10^9 t yr^{-1} (Syvitski and Kettner, 2011).

6. Conclusions

Direct measurements coupled with ^{7}Be and ^{210}Pb geochronology reveal that the 'abandoned' lower Ganges–Brahmaputra delta plain is actively accreting from a mix of flood pulse sediment and older sediment reworked from the shelf or tidal channel beds. This study presents a first-order approximation of spatial and temporal patterns of modern sedimentation on the lower Ganges–Brahmaputra delta and demonstrates that:

1. Patterns of sedimentation are locally heterogeneous, although seasonal delivery of sediment is evenly distributed throughout all parts of the Sundarbans, resulting in an overall mean accretion rate of 1 cm yr^{-1}, which is equivalent to the mean rate of relative sea level rise estimated for the Bengal coast.
2. 63% of all sediment deposited on the tidal delta plain during the 2008 monsoon was derived from the flood pulse. This indicates sediment eroded within 6 months from the surface of the catchment or upper floodplain is the principal source of sediments annually accreting on the lower delta plain surface. Thus, annual river sediment discharge is a direct factor in maintaining the stability of the Sundarbans relative to the rate of sea-level rise.
3. Delivery of ^{7}Be- and ^{210}Pb$_{xs}$-tagged flood pulse sediment to the remote inland parts of the delta plain suggest that tidal flooding frequency and period of inundation is controlling sedimentation on this part of the delta, and that distance from the active river mouth has less of an influence on sediment accretion.

4. Sundarbans morphology has remained stable for the last millennium, despite documented interannual variability in river discharge. Sedimentation in the Sundarbans is tidally controlled and therefore may not be sensitive to fluctuations in sediment load discharge to the inner shelf.
5. The Sundarbans is a significant sink for G–B river sediment, potentially storing as much as 13% of the sediment annually discharged at the river mouth. This has implications for the volume of sediment estimated to reach the canyon, the Bengal Fan, and ultimately the global ocean. While this study and others (e.g. Allison and Kepple, 2001) appear to reasonably constrain sedimentation rates and patterns in the Sundarbans, there have been no analogous measurements made in the delta plain near the active river mouth estuary that receives the bulk of G–B sediment discharge. The role that this area of the delta plays in sediment storage, dispersal, and bypass to the deep sea remains unknown.

Acknowledgments

Special thanks to Nazrul Islam Bachchu for ground support in the Sundarbans; Jahangir Alam Liton and Mahfuz Khan for field assistance, and to Leslie Wallace Auerbach and Stephanie Higgins for help with data processing. We also thank Reide Corbett at East Carolina University for analyzing our suspended sediment samples on their gamma well detector. The paper benefitted from the helpful comments of three anonymous reviewers. This research was funded through National Science Foundation grant OCE-0630595.

Appendix A. Supplementary data

Supplementary data related to this article can be found at http://dx.doi.org/10.1016/j.ecss.2013.07.014.

References

Adame, M.F., Neil, D., Wright, S.F., Lovelock, C.E., 2010. Sedimentation within and among mangrove forests along a gradient of geomorphological settings. Estuarine, Coastal and Shelf Science 86, 21–30.
Aalto, R., Nittrouer, C.A., 2012. Pb-210 geochronology of flood events in large tropical river systems. Philosophical Transactions of the Royal Society A – Mathematical Physical and Engineering Sciences 370 (1966), 2040–2074.
Allison, M.A., 1998. Geologic framework and environmental status of the Ganges–Brahmaputra Delta. Journal of Coastal Research 14 (3), 826–836.
Allison, M.A., Kepple, E.B., 2001. Modern sediment supply to the lower delta plain of the Ganges–Brahmaputra River in Bangladesh. Geo-Marine Letters 21, 55–74.
Allison, M.A., Kahn, S.R., Goodbred, S.L., Kuehl, S.A., 2003. Stratigraphic evolution of the late Holocene Ganges–Brahmaputra lower delta plain. Sedimentary Geology 155, 317–342.
Barua, D.P., 1990. Suspended sediment movement in the estuary of the Ganges–Brahmaputra–Meghna River system. Marine Geology 91, 243–253.
Barua, D.K., Kuehl, S.A., Miller, R.L., Moore, W.S., 1994. Suspended sediment distribution and residual transport in the coastal ocean off the Ganges–Brahmaputra river mouth. Marine Geology 120 (1), 41–61.
Baskaran, M., 1995. A search for the seasonal variability on the depositional; fluxes of ^{7}Be and ^{210}Pb. Journal of Geophysical Research 100 (D2), 2833–2840.
Baskaran, M., Santschi, P.H., 1993. The role of particles and colloids in the transport of radionuclides in coastal environments of Texas. Marine Chemistry 43 (1–4), 95–114.
Baskaran, M., Ravichandran, M., Bianchi, T.S., 1997. Cycling of ^{7}Be and ^{210}Pb in a high POC, shallow, turbid estuary of south-east Texas. Estuarine, Coastal and Shelf Science 45 (2), 165–176.
Bonniwell, E.C., Matisoff, G., Whiting, P.J., 1999. Determining the times and particle transit in a mountain stream using fallout radionuclides. Geomorphology 27, 75–92.
Chowdhury, M.I., 1966. On gradual shifting of the Ganges from west to east in delta building operations. In: Proceedings UNESCO Symposium on Scientific Problems of Humid Tropical Zone Delta and Their Implications. University of Dacca, Dacca, pp. 35–39.
Coleman, J.M., 1969. Brahmaputra River: channel processes and sedimentation. Sedimentary Geology 3, 129–239.
Coleman, J.M., Roberts, H.H., Stone, G.W., 1998. Mississippi River delta: an overview. Journal of Coastal Research 14 (3), 698–716.
Cruz, R.V., Harasawa, H., Lal, M., Wu, S., Anokhin, Y., Punsalmaa, B., Honda, Y., Jafari, M., Li, C., Huu Ninh, N., 2007. Asia: climate change 2007: impacts, adaptation and vulnerability. In: Parry, M.L., Canziani, O.F., Palutikof, J.P., van der Linden, P.J., Hanson, C.E. (Eds.), Contribution of Working Group II to the Fourth Assessment Report of the Intergovernmental Panel on Climate Change. Cambridge University Press, Cambridge, UK, pp. 469–506.
Donato, D.C., Kauffman, J.B., Murdiyarso, D., Kurnianto, S., Stidham, M., Kanninen, M., 2011. Mangroves among the most carbon-rich forests in the tropics. Nature Geoscience 4, 293–297.
Ellison, A.M., Mukherjee, B.B., Karim, A., 2000. Testing patterns of zonation in mangroves: scale dependence and environmental correlates in the Sundarbans of Bangladesh. Journal of Ecology 88, 813–824.
Eysink, W.D., 1983. Basic Considerations on the Morphology and Land Accretion Potentials in the Estuary of the Lower Meghna River. Land Reclamation Project Technical Report no. 15. Bangladesh Water Development Board, p. 85.
Feng, H., Cochran, J.K., Hirschberg, D.J., 1999. ^{234}Th and ^{7}Be as tracers for the transport and dynamics of suspended particles in a partially mixed estuary. Geochimica et Cosmochimica Acta 63 (17), 2487–2505.
French, J.R., 1983. Numerical simulation of vertical marsh growth and adjustment to accelerated sea level rise, North Norfolk, U.K. Earth Surface Processes and Landforms 18, 63–81.
French, J.R., Spencer, T., 1993. Dynamics of sedimentation in a tide-dominated backbarrier salt marsh, Norfolk, UK. Marine Geology 110, 315–331.
Giri, C., Pengra, B., Zhiliang, Z., Singh, A., Tieszen, L.L., 2007. Monitoring mangrove forest dynamics of the Sundarbans in Bangladesh and India using multi-temporal satellite data from1973 to 2000. Estuarine, Coastal and Shelf Science 73, 91–100.
Goodbred Jr., S.L., 2003. Response of the Ganges dispersal system to climate change: a source-to-sink view since the last interstade. Sedimentary Geology 162 (1), 83–104.
Goodbred Jr., S.L., Kuehl, S.A., 1998. Floodplain processes in the Bengal Basin and the storage of Ganges–Brahmaputra river sediment: an accretion study using ^{137}Cs and ^{210}Pb geochronology. Sedimentary Geology 121, 239–258.
Goodbred Jr., S.L., Kuehl, S.A., 1999. Holocene and modern sediment budgets for the Ganges–Brahmaputra river system: evidence for highstand dispersal to flood-plain, shelf, and deep-sea depocenters. Geology 27 (6), 559–562.
Hanebuth, T.J.J., Kudrass, H.R., Linstädter, J., Islam, B., Zander, A.M., 2013. Rapid coastal subsidence in the central Ganges–Brahmaputra Delta (Bangladesh) since the 17th-century deduced from submerged salt-producing kilns. Geology. http://dx.doi.org/10.1130/G34646.1.
Hawley, N., Robbins, J.A., Eadie, B.J., 1986. The partitioning of beryllium-7 in fresh-water. Geochimica et Cosmochimica Acta 50 (6), 1127–1131.
He, Q., Walling, D.E., 1996. Use of fallout Pb-210 measurements to investigate longer-term rates and patterns of overbank sediment deposition on the flood-plains of lowland rivers. Earth Surface Processes and Landforms 21 (2), 141–154.
Jian, J., Webster, P.J., Hoyos, C.D., 2009. Large-scale controls on Ganges and Brahmaputra River discharge on intraseasonal and seasonal time-scales. Quarterly Journal of the Royal Meteorological Society 135, 353–370.
Koch, D., Jacob, D.J., Graustein, W.C., 1996. Vertical transport of tropospheric aerosols as indicated by ^{7}Be and ^{210}Pb in a chemical tracer model. Journal of Geophysical Research 18, 651–666.
Kuehl, S.A., Hariu, T.M., Moore, W.S., 1989. Shelf sedimentation off the Ganges–Brahmaputra river system: evidence for sediment bypassing to the Bengal Fan. Geology 17, 1132–1135.
Kuehl, S.A., Levy, B.M., Moore, W.S., Allison, M.A., 1997. Subaqueous delta of the Ganges–Brahmaputra river system. Marine Geology 144, 81–96.
Lynch, J.C., Meriwether, J.R., McKee, B.A., Vera-Herrera, F., Twilley, R., 1989. Recent accretion in mangrove ecosystems based on ^{137}Cs and ^{210}Pb. Estuaries 12 (4), 264–299.
Matisoff, G., Bonniwell, E.C., Whiting, P.J., 2002. Soil erosion and sediment sources in an Ohio watershed using Beryllium-7, Cesium-137, and Lead-210. Journal of Environmental Quality 31, 54–61.
Matisoff, G., Wilson, C.G., Whiting, P.J., 2005. The ^{7}Be/^{210}Pb ratio as an indicator of suspended sediment age or fraction new sediment in suspension. Earth Surface Processes and Landforms 30, 1191–1201.
Milliman, J.D., Syvitski, J.P.M., 1992. Geomorphic/tectonic control of sediment discharge to the ocean: the importance of small mountainous rivers. The Journal of Geology 100, 525–544.
Morris, J.T., Sundareshwar, P.V., Nietch, C.T., Kjerfve, B., Cahoon, D.R., 2002. Responses of coastal wetlands to rising sea level. Ecology 83 (10), 2869–2877.
Mullenbach, B.L., Nittrouer, C.A., 2000. Rapid deposition of fluvial sediment in the Eel Canyon, northern California. Continental Shelf Research 20 (16), 2191–2212.
Olsen, C.R., Larsen, I.L., Lowry, P.D., Cutshall, N.H., Nichols, M.M., 1986. Geochemistry and deposition of Be-7 in river-estuarine and coastal waters. Journal of Geophysical Research-Oceans 91 (C1), 896–908.
Olsen, C.R., Thein, M., Larsen, I.L., Lowry, P.D., Mulholland, P.J., Cutshall, N.H., Byrd, J.T., Windom, H.L., 1989. Plutonium, Lead-210, and carbon isotopes in the Savannah Estuary: riverborne versus marine sources. Environmental Science and Technology 23, 1475–1481.
Papa, F., Durand, F., Rossow, W.B., Rahman, A., Bala, S.K., 2010. Satellite altimeter-derived monthly discharge of the Ganga–Brahmaputra River and its seasonal to interannual variations from 1993 to 2008. Journal of Geophysical Research 115 (C12), C12013.
Papa, F., Bala, S.K., Pandey, R.K., Durand, F., Gopalakrishna, V.V., Rahman, A., Rossow, W.B., 2012. Ganga–Brahmaputra river discharge from Jason-2 radar

altimetry: an update to the long-term satellite-derived estimates of continental freshwater forcing flux into the Bay of Bengal. Journal of Geophysical Research-Oceans (1978–2012) 117 (C11).
Permanent Service for Mean Sea Level (PSMSL), 2002, 2005. www.psmsl.org.
Reed, D.J., 2002. Sea level rise and coastal marsh sustainability: geological and ecological factors in the Mississippi delta. Geomorphology 48, 233–243.
Saari, H., Schmidt, S., Castaing, P., Blanc, G., Sautour, B., Masson, O., Cochran, J.K., 2010. The particulate $^{7}Be/^{210}Pb_{xs}$ and $^{234}Th/^{210}Pb_{xs}$ activity ratios as tracers for tidal-to-seasonal particle dynamics in the Gironde estuary (France): implications for the budget of particle-associated contaminants. Science of the Total Environment 408, 4784–4794.
Shearman, P., Bryan, J., Walsh, J.P., 2013. Trends in deltaic change over three decades in the Asia-Pacific region. Journal of Coastal Research. http://dx.doi.org/10.2112/JCOASTRES-D-12-00120.
Somayajulu, Y.K., Murty, V.S.N., Sarma, Y.V.B., 2003. Seasonal and interannual variability of surface circulation in the Bay of Bengal from TOPEX/Poseidon altimetry. Deep-Sea Research II 50, 867–880.
Sommerfield, C.K., Nittrouer, C.A., Alexander, C.R., 1999. ^{7}Be as a tracer of flood sedimentation on the northern California continental margin. Continental Shelf Research 19, 335–361.
Steiger, J., Gurnell, A.M., Goodson, J.M., 2003. Quantifying and characterizing contemporary riparian sedimentation. River Research and Applications 19, 335–352.
Syvitski, J.P.M., Kettner, A.J., 2011. Sediment flux and the Anthropocene. Philosophical Transactions of the Royal Society A – Mathematical Physical and Engineering Sciences 369, 957–975.
Turekian, K.K., Benninger, L.K., Dion, E.P., 1983. Be-7 and Pb-210 total depositional fluxes at New Haven, Connecticut and at Bermuda. Journal of Geophysical Research-Oceans and Atmospheres 88 (NC9), 5411–5415.
Vegas-Vilarrúbia, T., Baritto, F., López, P., Meleán, G., Ponce, M.E., Mora, L., Gómez, O., 2010. Tropical histosols of the Lower Orinoco Delta, features and preliminary quantification of their carbon storage. Geoderma 155 (3–4), 280–288.
Wallbrink, P.J., Murray, A.S., 1993. Use of fallout radionuclides as indicators of erosion processes. Hydrological Processes 7, 297–304.
Wallbrink, P.J., Murray, A.S., 1996. Distribution and variability of Be-7 in soils under different surface cover conditions and its potential for describing soil redistribution processes. Water Resources Research 32 (2), 467–476.
Walsh, J.P., Nittrouer, C.A., 2004. Mangrove-bank sedimentation in a mesotidal environment with large sediment supply, Gulf of Papua. Marine Geology 208, 225–248.
Wang, K., Cornett, R.J., 1993. Distribution coefficients of ^{210}Pb and ^{210}Po in laboratory and natural aquatic systems. Journal of Paleolimnology 9, 179–188.
Xue, C.T., 1993. Historical changes in the Yellow-river delta, China. Marine Geology 113 (3–4), 321–330.